Kyvelou, P., Gardner, L. and Nethercot, D. A. (2017) Design of Composite Cold-Formed Steel Flooring Systems. Structures. 12, 242-252.

Design of Composite Cold-Formed Steel Flooring Systems

Pinelopi Kyvelou [a], Leroy Gardner [b], David A. Nethercot [c]

[a] Department of Civil Engineering, Imperial College London, SW7 2AZ, UK.
Email: pinelopi.kyvelou11@imperial.ac.uk. (Corresponding author)

[b] Department of Civil Engineering, Imperial College London, SW7 2AZ, UK.
Email: leroy.gardner@imperial.ac.uk

[c] Department of Civil Engineering, Imperial College London, SW7 2AZ, UK.
Email: d.nethercot@imperial.ac.uk

Abstract

Recently conducted experimental and numerical investigations have shown that mobilisation of composite action within systems comprising cold-formed steel beams and wood-based floorboards is feasible and can lead to substantial improvements in structural performance. However, no design rules have yet been established for these systems in order to allow the beneficial effect of composite action to be exploited. In this paper, proposals for the design of such systems are devised and their theoretical basis is presented. At the core of the proposals is the calculation of the attained degree of partial shear connection and the shear bond coefficient for the composite members as a function of the geometric and material properties of their components and connectors. The accuracy of the devised design method for the prediction of moment capacity and flexural stiffness is demonstrated through comparisons with the results of 12 physical tests and about 80 numerical simulations reported in the literature. The proposals provide practical design rules for composite cold-formed steel floor beams, which are suitable for incorporation into future revisions of the Eurocodes.

Keywords: cold-formed steel, composite action, degree of partial shear connection, shear bond coefficient, wood-based particle boards

1 Introduction

Conventional composite beams, comprising hot-rolled steel beams and reinforced concrete slabs, are designed so that both steel and concrete components are exploited to the greatest possible extent. The shear connection employed within a composite beam is crucial for the structural performance and integrity of the system, since this provides the bond between the individual components, preventing them from working independently and, hence, leading to enhancement of the load carrying capacity and stiffness of the system.

Assuming a concrete slab lying on a steel beam with no connection between them, no shear force can be transferred at their interface, leading to these two structural components working independently under flexure while slipping relatively to each other. If, for the same structural system, an adequate number of stiff connectors is provided to prevent relative slip between the structural components, the composite cross-section acts monolithically, with no slip occurring at the interface and with the two materials exploited to the greatest possible extent (full shear connection and interaction). Finally, if the connectors employed at the interface are not sufficient to provide full shear connection and not stiff enough to provide full interaction, the shear connection and interaction are said to be partial. In this case, some slip occurs at the interface, and the load-carrying capacity is limited by failure of the shear connection.

Full shear connection should not be confused with full shear interaction; the former is related to the strength of the longitudinal shear connection while the latter is related to its stiffness [1,2]. In the ideal scenario of a system with full shear connection, the number and strength of the employed fasteners is such that the ultimate load of the system is controlled by the moment resistance of the system, and not by the strength of the connection; in case this cannot be achieved, the shear connection is referred to as partial [3]. In a system with full shear interaction, the two components act as a monolithic beam since the longitudinal slip between its components has been completely eliminated. Although full shear connection can be practically attained provided that enough shear connectors are employed within a composite system, it is unrealistic for full shear interaction to be achieved, since fasteners will always undergo some degree of deformation as they are loaded.

Recently conducted experimental and numerical research has shown that significant benefits are to be gained by mobilising composite action within floor systems comprising cold-formed steel beams and wood-based floorboards [4,5], an example of which is shown in Figure 1 [4,6]. However, no design rules have yet been established for these floors in order to exploit the beneficial effect of composite action on their structural performance. In this paper, proposals are made for the design of composite cold-formed steel flooring systems. Design expressions are presented for the calculation of the attained degree of shear connection and shear bond coefficient of a system, and for the determination of bending resistance, shear resistance and flexural stiffness (for deflection and vibration checks). The theoretical background of the employed equations is fully described, and the accuracy of the proposals is assessed against results obtained from physical tests and numerical analyses, reported in [4] and [5], respectively.

2 Moment resistance of composite systems

An analytical method, the core of which comprises the determination of the degree of partial shear connection, has been developed for the prediction of the moment capacity of a composite cold-formed steel flooring system. The proposed method, which is described in the following sub-sections, has been validated against experimental and numerical data reported in the literature [4,5] and was found to be capable of yielding accurate predictions of the gains in moment capacity of composite cold-formed steel flooring systems with partial shear connection.

2.1 Attained degree of shear connection

For a composite system (see Figure 2(a)) with full shear connection, the number of fasteners provided is such that the full plastic bending resistance can be achieved with the material strengths exploited to their greatest extent – see Figure 2(b). Otherwise, if the fasteners provided are fewer than those required for full shear connection, failure, controlled by the resistance of the connection, as shown in Figure 2(c), occurs earlier; in this case, the shear connection is partial.

Following the basic principles of Clause 6.6.3.1(1) of EN 1994-1-1 [7], the longitudinal force Q that can be withstood and, therefore, transferred by the shear connector of a composite

beam is limited either by the shear strength of the fastener P_v or by the bearing resistance of the board P_b in contact with the fastener. The values of P_b and P_v for the composite systems examined herein can be either determined from Equations (1) and (2), respectively [4] or obtained from push-out tests.

$$P_b = \frac{t_b\, d\, f_{cbd}}{\gamma_{M2}} \tag{1}$$

$$P_v = \frac{1}{\gamma_{M2}}\ \frac{\pi\, d_{thr}^{\,2}}{4}\ \frac{f_u}{\sqrt{3}} \tag{2}$$

where t_b and f_{cbd} are the thickness and the design compressive strength of the floorboard, respectively, d is the diameter of the employed connectors, d_{thr} is the threaded diameter of the connectors, usually equal to $0.75d$, f_u is the ultimate tensile strength of the steel fasteners and γ_{M2} is a partial safety factor with a recommended value of 1.25 [8].

Hence, Q may be determined from:

$$Q = \min\,(P_b, P_v) \tag{3}$$

For a fully composite system, the resistance of the employed connection is greater than the longitudinal force generated at the critical cross-section of the beam by the applied bending moment such that the bending resistance of the critical cross-section can be attained prior to failure of the shear connection. Therefore, the force carried by the shear connection at the beam-board interface V_l (determined from Equation (4)), which, as shown in Figure 3, equals the total force developed in the slab, is limited either by the compressive strength of the wood-based board C_b or by the tensile strength of the steel beam T_s, as determined from Equations (5) and (6), respectively.

$$V_l = \min(C_b, T_s) \tag{4}$$

$$C_b = A_b f_{cbd} \tag{5}$$

$$T_s = A_s f_y / \gamma_{M0} \tag{6}$$

where A_b and A_s are the areas of the flooring panel and steel beam, respectively, f_y is the yield strength (0.2% proof strength) of the cold-formed steel beam with $\gamma_{M0} = 1.0$ [9] and f_{cbd} is the design compressive strength of the floorboard material, taken as:

$$f_{cbd} = f_{cb}/\gamma_M \quad (7)$$

with γ_M = 1.3, according to Table 2.3 of EN 1995-1-1 [10]. Note that the typical spacing of cold-formed steel beams employed for the examined flooring systems is 600 mm. Since the conducted experiments and numerical simulations have shown no evidence of shear lag for this spacing [4,5], the effective width of the floorboard b_{eff} can be taken equal to the spacing of the beams (i.e. 600 mm). The area of the flooring panel A_b may therefore be taken as the product of the effective width of the floorboard b_{eff} and the thickness of the floorboard t_b ($A_b = t_b\ b_{eff}$). Further investigation would be required for systems with wider beam spacings. The origin of Equation (4) can be explained with reference to the position of the plastic neutral axis (PNA) along the height of the composite cross-section, as shown in Figure 3, according to the three possible scenarios described below:

a) $C_b = T_s \therefore$ PNA lies at the beam-board interface (Figure 3(a)) and

$$V_l = C_b = T_s \quad (8)$$

b) $C_b > T_s \therefore$ PNA lies in the floorboard (Figure 3(b)) and

$$V_l = T_s = C_{b,c} - C_{b,t} \quad (9)$$

c) $C_b < T_s \therefore$ PNA lies in the steel beam (Figure 3(c)) and

$$V_l = C_b = T_{s,t} - T_{s,c} \quad (10)$$

where $C_{b,c}$ and $C_{b,t}$ are the compressive and tensile forces developed in the board when the neutral axis lies within it while, when it lies within the steel beam, the corresponding compressive and tensile forces developed in the steel beam are $T_{s,c}$ and $T_{s,t}$, respectively. Note that the spacing of the cold-formed steel beams employed for the examined flooring systems is 600 mm. Since, according to the conducted experiments and numerical simulations [4,5], no shear lag effects have been observed for this spacing, the effective width of the floorboard b_{eff} can be taken equal to the spacing of the beams (i.e. 600 mm). Further investigation would be required for systems with wider beam spacings.

EN 1994-1-1 [7] allows uniform spacing of fasteners along all critical lengths of a composite beam, defined as the lengths between two critical cross-sections, such as sections of maximum bending moment and sections subjected to high concentrated forces (positions of point loads and supports) [11]. Hence, for a fully composite system, the number of shear connectors $n_{f,cr}$ required along each critical length of the beam is:

$$n_{f,cr} = \frac{V_l}{Q} \tag{11}$$

For a single-span composite beam subjected to uniformly distributed load, there are two critical lengths requiring $n_{f,cr}$ number of connectors; each one is defined by the distance between the support and the midspan cross-section. Hence, the number of shear connectors n_f required along the full length of the beam is:

$$n_f = 2\, n_{f,cr} \tag{12}$$

Therefore, for a flooring system with n connectors in the critical lengths, the attained degree of shear connection η_d is given by:

$$\eta_d = \frac{n}{n_f} \leq 1 \tag{13}$$

2.2 Calculation of moment resistance

According to Clause 6.2.1.3(3) of EN 1994-1-1 [7], for steel beams with Class 1 or 2 cross-sections, the moment capacity of a composite system with partial shear connection $M_{pl,Rd}$ varies between the plastic moment capacity of the bare steel beam $M_{pl,bare}$ and the plastic moment capacity of the fully composite beam $M_{pl,comp}$, and can be calculated using either by the conservative linear interpolation method or by the equilibrium method, as shown in Figure 4.

Note that the derivation of the moment capacity of the fully composite system $M_{pl,comp}$ depends on the position of the plastic neutral axis within the depth of the composite cross-section. There are three possible scenarios, as illustrated in Figure 3:

1) <u>The plastic neutral axis is located at the beam-board interface.</u>

   In this case, the plastic moment resistance of the composite section $M_{pl,comp}$ can be calculated according to Equation (14), by taking moments about the axis of the tensile force T_s in the steel beam (see Figure 3(a)):

$$M_{pl,comp} = A_b f_{cbd} \left(\frac{h}{2} + \frac{t_b}{2} \right) \tag{14}$$

   where A_b is the area of the floorboard and f_{cbd} is its design compressive strength.

2) <u>The plastic neutral axis is located in the floorboard.</u>

In this case, the plastic moment resistance of the composite section $M_{pl,comp}$ can be calculated according to Equation (15), by taking moments about the axis of the tensile force T_s in the steel beam (see Figure 3(b)):

$$M_{pl,comp} = A_{b,c} f_{cbd} \left(\frac{h}{2} + t_b - \frac{x}{2} \right) - A_{b,t} f_{tbd} \left(\frac{h}{2} + \frac{t_b - x}{2} \right) \quad (15)$$

where $A_{b,c}$ and $A_{b,t}$ are the areas of the floorboard in compression and tension, respectively, f_{cbd} and f_{tbd} are the designcompressive and tensile strengths of the board, respectively while x is the distance of the plastic neutral axis from the top fibre of the composite section.

3) <u>The plastic neutral axis is located in the steel beam.</u>

In this case, the plastic moment resistance of the composite section $M_{pl,comp}$ can be calculated according to Equation (16), by taking moments about the axis of the tensile force $T_{s,t}$ in the steel beam (see Figure 3(c)):

$$M_{pl,comp} = A_b f_{cbd} \left(\frac{t_b}{2} + h - y_{s,t} \right) + A_{s,c} f_y \left(y_{s,c} - y_{s,t} \right) \quad (16)$$

where $A_{s,c}$ is the area of the steel beam under compression, f_y is its yield strength and $y_{s,c}$ and $y_{s,t}$ are the distances from the bottom fibre of the composite section to the centroids of the parts of the steel beam in compression and in tension, respectively.

Finally, the plastic moment capacity of the bare steel beam $M_{pl,bare}$ is given by:

$$M_{pl,bare} = \frac{A_s}{2} f_y z \quad (17)$$

where z is the distance between the centroids of the parts of the steel beam under tension and compression.

Since cold-formed steel sections are typically Class 3 or Class 4, their cross-sectional moment resistance M_{bare} is limited, due to their susceptibility to local instabilities, to the elastic or an effective moment capacity, which can be calculated in accordance with EN 1993-1-3 (2006) and EN 1993-1-5 [12], while their plastic moment resistance $M_{pl,bare}$ cannot be attained. However, if full shear connection is provided, leading to the board being fully engaged, $M_{pl,comp}$ often can be attained. This can be explained with reference to the position of the neutral axis which, for a fully composite beam, moves up the composite cross-sectional depth with increasing shear connection, allowing the steel cross-section to work mainly, if

not completely, under tension. Note that, for all the systems examined within this paper, when full shear connection is assumed, all the cross-sections are classified as Class 1 [9].

Hence, according to the proposed design method, the moment resistance of a composite cold-formed steel flooring system $M_{c,Rd}$ ranges between the moment resistance of the bare steel beam M_{bare} when $\eta_d = 0$ and the moment resistance of the fully composite beam $M_{pl,comp}$ when $\eta_d = 1$, following curve A'-C presented in Figure 5. Curve A'-C is derived by scaling the capacity down from $M_{pl,bare}$ to M_{bare} at $\eta_d = 0$, then applying a linearly decreasing reduction to $M_{pl,Rd}$, down to zero change at $\eta_d = 1$. For example, for a system with a degree of partial shear connection of $\eta_d = 0.1$, the plastic moment capacity assuming a plastic distribution of stresses $M_{pl,Rd}$ can be calculated based on the equilibrium of forces within the cross-section, represented by point B on curve A-C of Figure 5. Then, in order to calculate the actual moment resistance $M_{c,Rd}$ of the system (point B' on curve A'-C), it is assumed that $M_{pl,Rd}$ is reduced by 90% of the difference between $M_{pl,bare}$ and M_{bare}. The moment capacity of a composite beam $M_{c,Rd}$ with an attained degree of partial shear connection η_d can therefore be calculated according to Equation (18):

$$M_{c,Rd} = M_{pl,Rd} - (1 - \eta_d)\,(M_{pl,bare} - M_{bare}) \tag{18}$$

Note that $M_{pl,Rd}$ is the moment capacity of a system with the same degree of partial shear connection as the examined system, derived based on the equilibrium method (point B) assuming a plastic distribution of stresses.

An alternative, more conservative approach to calculate the moment capacity of the composite system is to interpolate between points A' and C of Figure 5:

$$M_{c,lin,Rd} = M_{bare} + \eta_d\,(M_{pl,comp} - M_{bare}) \tag{19}$$

It should be mentioned that the methods described herein can be used only for systems for which, when full shear connection is assumed, the composite section is classified as Class 1 or 2 – see Table 5.2 of EN 1993-1-1 [9] – so the assumption that $M_{pl,comp}$ can be reached, is valid. In case this limitation is not fulfilled (i.e. if the fully composite section is Class 3), it is suggested that the moment capacity of the composite system is taken equal to the capacity of the bare steel beam; further research is required in order for the composite action arising within a Class 3 composite section to be taken into consideration in design.

2.3 Shear buckling resistance

Although the mobilisation of composite action within the examined flooring systems can have a significant influence on the cross-sectional moment capacity, the shear buckling resistance $V_{b,Rd}$ depends only on the bare steel beam. Thus, for the examined cold-formed steel beams, $V_{b,Rd}$ is calculated according to Clause 6.1.5 of EN 1993-1-3 [8]:

$$V_{b,Rd} = \frac{\frac{h_w}{\sin\varphi}\, t f_{bv}}{\gamma_{M0}} \tag{20}$$

where f_{bv} is the shear strength considering buckling according to Table 6.1 of EN 1993-1-3 [8], h_w is the web height between the midlines of the flanges, φ is the slope of the web relative to the flanges and γ_{M0} is the partial factor for the resistance of cross-sections [8].

2.4 Interaction between bending and shear

Degradation of the moment resistance with high levels of shear can be observed in Figure 6, where the applied moment M_{Ed} normalised by the moment capacity $M_{c,Rd}$ is plotted against the applied vertical shear force V_{Ed} normalised by the shear resistance $V_{b,Rd}$ for all the conducted physical tests and numerical simulations presented in [4] and [5], respectively. It is evident that an appropriate allowance should be made, accounting for the effect of high shear force on the moment resistance $M_{c,Rd}$. Hence, following the same principles employed in EN 1994-1-1 [7] and EN 1993-1-1 [9], a reduction in $M_{c,Rd}$, according to Equation (21) (plotted in Figure 6 for a typical section), is proposed for systems where the value of V_{Ed} exceeds half the value of the shear resistance $V_{b,Rd}$. Note that $M_{f,Rd}$, determined as the moment resistance of the composite cross-section consisting of the effective flanges only and no web, provides a lower bound to the bending resistance M_{Rd} due to interaction of bending and shear.

$$M_{Rd} = M_{f,Rd} + (1-\rho)\left(M_{c,Rd} - M_{f,Rd}\right) \tag{21}$$

where:

$$\rho = \begin{cases} \left(2\frac{V_{Ed}}{V_{b,Rd}} - 1\right)^2 & \text{for } V_{Ed} / V_{b,Rd} \geq 0.5 \\ 0 & \text{for } V_{Ed} / V_{b,Rd} < 0.5 \end{cases} \tag{22}$$

2.5 Minimum allowed degree of partial shear connection

A basic requirement for equally spaced shear connectors along the length of a composite beam is that their deformation capacity is such that sufficient redistribution of the longitudinal shear force at the beam-board interface can be achieved for all connectors to be approximately equally loaded under flexure despite the slip near the ends of the beam being higher than that close to midspan [13].

The deformation capacity and hence the ductility of a connector is directly related to its slip capacity, defined as the maximum slip that can be withstood with no loss of resistance of the connector; this can be established from push-out tests. For conventional steel-concrete composite beams, in order for a connector to be classified as ductile, a characteristic slip capacity of at least 6 mm is required [7,14] while, in order for plastic design to be employed, a minimum degree of partial shear connection is defined.

The lower bound limit for the degree of partial shear connection reflects the need for the shear connectors to remain elastic under serviceability loading, thus preventing the development of cumulative, inelastic deformations. Therefore, as underlined in [15], this resistance check is indirectly checking the stiffness at the shear interface. For conventional steel-concrete composite construction and based on experimental data, a minimum value of 40% shear connection (i.e. η_d = 0.4) has been established as the minimum required limit above which the assumption of a ductile shear connection is acceptable and, hence, plastic design can be safely employed [7,14]. However, while a lower bound limit of partial shear connection is required for the reasons described above, it has been shown that the 40% limit currently employed in design standards is over conservative, leading, in some cases, to uneconomical composite solutions [15,16].

In Figure 7, the deformations at ultimate load s_u exhibited by the connectors of two typical systems examined within this paper are plotted against the length of the beam while, in Figure 8, the ratio of the maximum force $P_{u,max}$ to the minimum force $P_{u,min}$ experienced by the connectors located in the critical lengths are plotted against the corresponding attained degree of shear connection of the system η_d. For the composite flooring systems examined within this paper, with increasing degree of shear connection, the deformation of the connectors located near the ends of the beam decreases while, for values of η_d greater than 0.05, the variation of the ratio $P_{u,max}/P_{u,min}$ remains relatively constant. Note that the data

presented in Figures 7 and 8 were obtained from numerical simulations presented in detail in [5] and refer to single-span composite beams subjected to four-point bending.

It is therefore proposed that the moment capacity M_{Rd} of a composite cold-formed steel flooring system should be obtained following the procedure described in Sections 2.2 – 2.4 for degrees of partial shear connection exceeding the value of $\eta_d = 0.05$, but for $\eta_d < 0.05$ composite action should not be taken into consideration and the moment capacity of the system M_{Rd} should be taken equal to the moment capacity of the bare steel beam M_{bare}, as given by Equation (23). Note that in order to fully establish the validity of the 5% lower bound limit adopted herein, further investigation is required examining alternative fasteners and loading configurations.

$$M_{Rd} = \begin{cases} M_{f,Rd} + (1-\rho)\left(M_{c,Rd} - M_{f,Rd}\right) & \text{for } \eta_d \geq 0.05 \\ M_{bare} & \text{for } \eta_d < 0.05 \end{cases} \quad (23)$$

2.6 Summary of proposed design method for the determination of moment capacity

The proposed design approach for determining the moment and shear capacity of a cold-formed steel composite floor beam is summarised into the following steps:

a) Calculate the design values for bending moment M_{Ed} and shear force V_{Ed} from the applied factored loads.

b) Calculate the attained degree of shear connection η_d from Equation (13).

c) Calculate the moment capacity of the system, accounting for composite action $M_{c,Rd}$ from Equation (18) or (19).

d) Calculate the shear resistance of the steel section $V_{b,Rd}$ from Equation (20).

e) Check that $V_{Ed} / V_{b,Rd} \leq 1$.

f) Calculate the reduction factor ρ accounting for the reduction of bending moment capacity due to the presence of high shear forces from Equation (22).

g) Calculate the bending resistance of the composite system in the presence of shear M_{Rd} from Equation (23).

h) Check that $M_{Ed} / M_{Rd} \leq 1$.

2.7 Comparison of design proposal with experimental and numerical data

Table 1 presents comparisons between the ultimate moment capacities M_{Rd} and $M_{lin,Rd}$ predicted by the equilibrium and interpolation design methods, respectively and those obtained from 8 physical tests [4] and 78 numerical simulations [5] M_u, with a mean M_{Rd}/M_u ratio of 0.91 and a mean $M_{lin,Rd}/M_u$ ratio of 0.86. Note that, for the comparisons presented in Table 1, the specimens are categorised accoprding to the employed spacing of fasteners s_f while the predicted ultimate moment capacities M_{Rd} and $M_{lin,Rd}$ have been derived using measured (or modelled) geometric and material properties, as reported in [4] and [5], with all partial safety factors taken equal to unity.

In Figure 9, the gains in capacity due to composite action for all systems, normalised by the capacities corresponding to the equivalent bare steel and fully composite systems, as predicted from the proposed equilibrium design method and as observed in the conducted experiments and numerical analyses [4,5], are plotted against the corresponding attained degrees of shear connection, with zero on the vertical axis being the capacity of the bare steel section M_{bare} and unity being the capacity of the fully composite section $M_{pl,comp}$. It can be observed that the proposed design method gives accurate and generally safe-side predictions for the gains in moment capacity of a composite system with different degrees of partial shear connection.

3 Flexural stiffness of composite systems

Current design methods for conventional steel-concrete composite structures do not include an explicit formula for the prediction of the effective flexural stiffness of a system with partial interaction. Numerical and experimental results have shown that, although the flexural stiffness of the fully composite system $(EI)_{comp}$ cannot be practically attained – and hence the assumption of full shear interaction is unsafe – the benefits in flexural stiffness gained due to the mobilisation of composite action are too significant to be ignored.

An analytical method, which has been developed for the prediction of the effective flexural stiffness of a system with partial shear interaction, is presented herein. The proposed method, described in the following sub-sections, has been validated against data obtained both from physical tests and numerical analyses [4,5] and was found capable of accurately predicting the gains in flexural stiffness for composite cold-formed steel flooring systems with partial shear interaction.

3.1 Determination of shear bond coefficient

In Section B.2 of Annex B of EN 1995-1-1 [10], a formula is given for the calculation of the effective bending stiffness of mechanically jointed beams made of timber, the derivation of which has been presented in [17]. An equivalent formula for calculating the effective flexural stiffness of composite cold-formed steel − wood flooring systems is derived herein, following the same general approach.

For the simply supported beam of span L shown in Figure 10(a), the slip modulus of the shear connection along the beam-board interface is denoted k. The area of the board and steel beam are denoted A_b and A_s, respectively while their second moments of area are denoted I_b and I_s, respectively. When subjected to vertical load, the beam deforms, as shown in Figure 10(b) and, as a result, the longitudinal shear forces developed at the interface are resisted by the shear connection.

Examining the internal forces acting on an incremental element of beam of length dx, as shown in Figure 10(c), we obtain, from equilibrium of horizontal (axial) forces and moments acting on the board:

$$\mathrm{d}N_b + v_l \,\mathrm{d}x = 0 \therefore N_b' + v_l = 0 \tag{24}$$

$$\mathrm{d}M_b = V_b \,\mathrm{d}x - v_l \,\mathrm{d}x \,\frac{t_b}{2} \therefore M_b' = V_b - v_l \,\frac{t_b}{2} \tag{25}$$

Accordingly, from equilibrium of horizontal forces and moments acting on the steel section:

$$\mathrm{d}N_s - v_l \,\mathrm{d}x = 0 \therefore N_s' - v_l = 0 \tag{26}$$

$$\mathrm{d}M_s = V_s \,\mathrm{d}x - v_l \,\mathrm{d}x \,\frac{h}{2} \therefore M_s' = V_s - v_l \,\frac{h}{2} \tag{27}$$

Finally, from equilibrium of vertical (shear) forces:

$$\mathrm{d}V_\mathrm{b} + \mathrm{d}V_\mathrm{s} = -q\,\mathrm{d}x \therefore V' = V_\mathrm{b}' + V_\mathrm{s}' = -q \tag{28}$$

where v_l is the shear force per unit length acting continuously along the beam-board interface, N, V and M are the axial forces, shear forces and bending moments, respectively while the subscripts b and s represent the board and steel section, respectively. The primes represent differentiation with respect to x, for instance $N' = \frac{\mathrm{d}N}{\mathrm{d}x}$.

Differentiation of the sum of Equations (25) and (27) with respect to x gives:

$$M_\mathrm{b}'' + M_\mathrm{s}'' + v_\mathrm{l}'\,\alpha + q = 0 \tag{29}$$

where, as shown in Figure 10(d):

$$\alpha = \frac{t_\mathrm{b} + h}{2} \tag{30}$$

As shown in Figure 10(d), the vertical deflection of the beam due to the applied vertical load q is denoted w, and the angle of rotation θ of the cross-section about its centroid due to bending, assuming small angles, is:

$$\theta \approx w' \approx \tan^{-1}(w') \tag{31}$$

Hence, as shown in Figure 10(d), the relative horizontal slip u that has to be withstood by the connection at the beam-board interface is:

$$u = u_\mathrm{s} - u_\mathrm{b} + w'\,\alpha \tag{32}$$

Thus, the longitudinal force per unit length v_l that has to be transferred by the shear connection is:

$$v_\mathrm{l} = k\,u = k\,(u_\mathrm{s} - u_\mathrm{b} + w'\,\alpha) \tag{33}$$

From elastic bending theory:

$$N_\mathrm{b} = E_\mathrm{b}\,A_\mathrm{b}\,u_\mathrm{b}' \quad , \quad N_\mathrm{s} = E_\mathrm{s}\,A_\mathrm{s}\,u_\mathrm{s}' \tag{34}$$

$$M_\mathrm{b} = -E_\mathrm{b}\,I_\mathrm{b}\,w'' \quad , \quad M_\mathrm{s} = -E_\mathrm{s}\,I_\mathrm{s}\,w'' \tag{35}$$

$$V_\mathrm{b} = -E_\mathrm{b}\,I_\mathrm{b}\,w''' \quad , \quad V_\mathrm{s} = -E_\mathrm{s}\,I_\mathrm{s}\,w''' \tag{36}$$

Substitution of Equations (33) – (36) in Equations (24), (26) and (29) gives:

$$E_b\, A_b\, u_b'' + k\,(u_s - u_b + w'\,\alpha) = 0 \tag{37}$$

$$E_s\, A_s\, u_s'' - k\,(u_s - u_b + w'\,\alpha) = 0 \tag{38}$$

$$(E_b I_b + E_s I_s)\, w'''' - k\,\alpha\,(u_s' - u_b' + w''\,\alpha) = q \tag{39}$$

For a sinusoidal distribution of the vertical load q, the shapes of the deformations u_b, u_s and w, as defined in Figure 10(a), are given by the following sinusoidal functions:

$$q = q_o \sin\left(\frac{\pi}{L}x\right) \tag{41}$$

$$u_b = u_{bo} \cos\left(\frac{\pi}{L}x\right) \tag{42}$$

$$u_s = u_{so} \cos\left(\frac{\pi}{L}x\right) \tag{43}$$

$$w = w_o \sin\left(\frac{\pi}{L}x\right) \tag{44}$$

Substitution of Equations (40) – (43) in Equations (37) – (39), leads to a system of three equations including the constants q_o, u_{bo}, u_{so} and w_o. Solving the resulting system of equations for w_o yields:

$$w_o = q_o\, \frac{L^4}{\pi^4}\, \frac{1}{E_b I_b + E_s I_s + \dfrac{E_b\, A_b\, E_s\, A_s\, \alpha^2}{E_s\, A_s\, \dfrac{\pi^2}{L^2}\, \dfrac{E_b\, A_b}{k} + E_b A_b + E_s A_s}} \tag{44}$$

This may be expressed in the more familiar format:

$$w_o = q_o\, \frac{L^4}{\pi^4}\, \frac{1}{(EI)_{eff}} \tag{45}$$

with the effective flexural stiffness of the examined composite beam given by:

$$(EI)_{eff} = E_b I_b + E_s I_s + \frac{E_b\, A_b\, \gamma\, \alpha^2}{1 + \gamma\, \dfrac{E_b\, A_b}{E_s A_s}} \tag{46}$$

where k is the slip modulus of the shear connection and is calculated according to Equation (47) as a function of the slip modulus K_o and spacing s_f of the employed fasteners while γ, given by Equation (48), is the shear bond coefficient.

$$k = \frac{K_o}{s_f} \tag{47}$$

$$\gamma = \frac{1}{1 + \frac{\pi^2}{L^2} \frac{E_b A_b}{k}} \quad (48)$$

Note that, although a sinusoidal distribution of the vertical load has been assumed, the derived formula has been found to be capable of accurately predicting the effective flexural stiffness of beams subjected to most other common loading distributions [17].

3.2 Comparison of design proposal with experimental and numerical data

Table 1 presents comparisons between values of flexural stiffness $(EI)_{eff}$ predicted by the design method based on the shear bond coefficient γ and those obtained from physical tests and numerical simulations EI reported in the literature [4,5], with a mean $(EI)_{eff}$ /EI ratio of 1.01 and a COV of 0.02.

Note that, for the derivation of the values of $(EI)_{eff}$, L was taken equal to the sum of the critical lengths of the beams ($2L/3$) due to the adopted four-point bending configuration employed in the test and FE arrangements, with zero shear force in the central third of the beam. For a beam under a uniformly distributed load (udl), L would be equal to the full length of the beam.

A comparison between the predicted EI values and the actual values obtained from experimental and numerical investigations [4,5] is graphically illustrated in Figure 11, where the ratio of $(EI)_{eff}$ /EI is plotted against the shear bond coefficient γ of each system. It can be observed that the devised method is capable of accurately predicting the effective flexural stiffness of composite systems with partial interaction.

4 Worked example

A 6 m long single-span flooring system comprising cold-formed steel beams and wood-based floorboards is shown in Figure 12. The floor is loaded such that each beam is subjected to uniformly distributed load comprising a dead load of 1.4 kN/m and a live load of 2.0 kN/m. The beams are stiffened at the ends with cleat connections. The employed shear connectors are self-drilling screws, the spacing s_f of which is 140 mm. The geometrical and material characteristics of the steel sections and the wood-based panels are reported in Tables 2 and 3, respectively while the characteristics of the employed fasteners are listed in Table 4. The

moment capacity of the bare steel section M_{bare} = 18.73 kNm. The beam is to be checked for bending, shear and deflections.

4.1 Moment resistance

a) For ultimate limit state design, the design load q_d is:

$q_d = 1.35 \times 1.4 + 1.50 \times 2.0 = 4.89$ kN/m

Therefore, the design shear force V_{Ed} and the design bending moment M_{Ed} are:

$$M_{Ed} = \frac{q_d L^2}{8} = 22.01 \text{ kNm}$$

$$V_{Ed} = \frac{q_d L}{2} = 14.67 \text{ kN}$$

b) The bearing resistance P_b of the floorboard and the shear strength of each fastener P_v are calculated from Equations (1) and (2), respectively:

$$P_b = \frac{t_b \, d \, f_{cbd}}{\gamma_{M2}} = 1.66 \text{ kN}$$

$$P_v = \frac{1}{\gamma_{M2}} \frac{\pi \, d_{thr}^{\,2}}{4} \frac{f_u}{\sqrt{3}} = 4.44 \text{ kN}$$

Note that, according to Equation (7): $f_{cbd} = f_{cb} / \gamma_M = 12.9 / 1.3 = 9.92$ MPa.

Hence, according to Equation (3), the strength Q of the shear connection is:

$Q = \min(P_b , P_v) = 1.66$ kN

For the fully composite system, the longitudinally transferred shear force V_l , calculated according to Equation (4), must be limited either by the compressive strength of the wood-based board C_b or by the tensile strength of the steel beam T_s, as determined from Equations (5) and (6), respectively:

$C_b = A_b \, f_{cbd} = 226.25$ kN

$T_s = A_s \, f_y / \gamma_{M0} = 321.60$ kN

$V_l = \min(C_b , T_s) = 226.25$ kN

Hence, according to Equations (11) and (12), in order to achieve full shear connection, the required number of fasteners n_f is:

$$n_f = 2 \frac{V_l}{Q} = 2 \frac{226.25}{1.66} = 2 \times 137 = 274 \text{ fasteners}$$

The number of employed fasteners n along the critical lengths of the examined system is:

$n = L / s_f = 42$ fasteners

Therefore, the attained degree of shear connection η_d from Equation (13) is:

$$\eta_d = \frac{n}{n_f} = 0.15 \leq 1$$

c) The moment capacity of the bare steel section is:

$M_{bare} = 18.73$ kNm

For the theoretical fully composite system, since $C_b < T_s$, the plastic neutral axis lies in the steel beam. More specifically, from cross-sectional equilibrium, the plastic neutral axis of the fully composite section may be shown to lie within the top flange of the steel beam. Hence, with the neutral axis lying on the top flange of the steel section and restrained by the shear connection, and the remainder of the steel beam being subjected to tension, the fully composite section is classified as Class 1. Thus, the moment capacity of the examined system assuming full shear connection is:

$M_{pl,comp} = 43.87$ kNm

The moment capacity of the bare steel section assuming a plastic distribution of stresses is:

$M_{pl,bare} = 27.57$ kNm

And, from cross-sectional equilibrium, the plastic moment capacity corresponding to 15% of partial shear connection ($\eta_d = 0.15$) is:

$M_{pl,Rd} = 32.06$ kNm

Hence, according to the proposed design method, the moment resistance of the examined composite system $M_{c,Rd}$ is calculated according to Equation (18):

$M_{c,Rd} = M_{pl,Rd} - (1 - \eta_d) (M_{pl,bare} - M_{bare}) = 24.58$ kNm

A schematic illustration of the moment capacities required for the calculation of the moment resistance of the composite system $M_{c,Rd}$ is shown in Figure 13.

4.2 Shear resistance

d) Following the procedure described in Clause 6.1.5(1) of EN 1993-1-3 [8], the design shear resistance $V_{b,Rd}$ of a cold-formed steel section is calculated according to Equation (20):

$$V_{b,Rd} = \frac{\frac{h_w}{\sin\varphi}\, t f_{bv}}{\gamma_{M0}}$$

where: $\gamma_{M0} = 1.00$ according to Clause 2(3) of EN 1993-1-3 [8]

$h_w = 248.5$ mm is the web height between midlines of flanges

$\varphi = 90^o$ is the slope of the web relative to the flanges

f_{bv} is the shear buckling strength, obtained from Table 6.1 of Clause 6.1.5(1) According to Table 6.1, and since the examined system is stiffened at the supports with cleats, the shear buckling strength can be calculated as follows:

$$f_{bv} = \begin{cases} 0.58 f_y & \text{, for } \bar{\lambda}_w \le 0.83 \\ 0.48 f_y / \bar{\lambda}_w & \text{, for } \bar{\lambda}_w > 0.83 \end{cases}$$

where $\bar{\lambda}_w$ is the slenderness of the steel web.

According to Equation 6.10(b) of EN 1993-1-3 [8], the relative web slenderness $\bar{\lambda}_w$ for webs with longitudinal stiffeners is:

$$\bar{\lambda}_w = 0.346 \frac{s_d}{t} \sqrt{\frac{5.34}{k_\tau} \frac{f_y}{E_s}} \ge 0.346 \frac{s_p}{t} \sqrt{\frac{f_y}{E_s}}$$

with $$k_\tau = 5.34 + \frac{2.10}{t} \left(\frac{\sum I_s}{s_d}\right)^{1/3}$$

where: $s_w = 248.5$ mm is the length of the web between corner midpoints

$s_p = 62.83$ mm is the length of the longest flat portion of the web

$s_d = 262.87$ mm is the total developed height of the web

I_s = 1753.73 mm^4 is the second moment of area of each individual stiffener, calculated in accordance with Figure 5.13 and Equations 5.32 and 5.33(a) of Clause 5.5.3.4.3 of EN 1993-1-3 [8]

Hence, the design shear resistance of the steel section is:

$V_{b,Rd}$ = 37.31 kN

e) $V_{Ed} / V_{b,Rd} = 0.39 \leq 1$

f) According to Section 2.4, and since $V_{Ed} / V_{b,Rd} = 0.39 < 0.50$, no reduction of the moment resistance of the composite section $M_{c,Rd}$ is required to account for shear forces.

Hence, according to Equation (22):

$\rho = 0$

g) According to Equation (23), the moment resistance of the composite system is:

M_{Rd} = 24.58 kNm

h) $M_{Ed} / M_{Rd} = 0.90 \leq 1$

Alternatively, if the design method based on linear interpolation between M_{bare} and $M_{pl,comp}$ is performed, step (c) of the present section is modified based on Equation (19):

$M_{Rd} = M_{c,lin,Rd} = (M_{bare} + \eta_d (M_{pl,comp} - M_{bare}) = 22.58$ kNm

$M_{Ed} / M_{lin,Rd} = 0.97 \leq 1$

4.3 Deflections

a) According to Equation (30): $\alpha = \frac{t_b + h}{2} = 144$ mm

b) The shear bond coefficient γ is calculated according to Equations (47) and (48):

$$\gamma = \frac{1}{1 + \frac{\pi^2}{L^2} \frac{E_{bd} A_b}{k}} = 0.44$$

c) The effective flexural stiffness of the composite system $(EI)_{eff}$ is calculated according to Equation (46):

$$(EI)_{\text{eff}} = E_{\text{bd}} I_{\text{b}} + E_{\text{s}} I_{\text{s}} + \frac{E_{\text{bd}} A_{\text{b}} \gamma \alpha^2}{1 + \gamma \frac{E_{\text{bd}} A_{\text{b}}}{E_{\text{s}} A_{\text{s}}}} = 1.48 \times 10^6 \text{ Nm}^2$$

For the deflection check, the design load q_{d} is taken equal to the unfactored imposed loads. Therefore:

$q_{\text{d}} = 2.0$ kN/m

The midspan deflection of the simply supported beam under q_{d} is:

$$\delta_{\max} = \frac{5 q_{\text{d}} L^4}{384 (EI)_{\text{eff}}} = 23 \text{ mm} < \frac{L}{200} = 30 \text{ mm}$$

The beam therefore passes the bending, shear and deflection checks, but would have failed in bending if composite action was ignored.

5 Conclusions

Design rules to harness composite action in steel-concrete systems are well established, but equivalent rules for steel-timber construction are lacking. This has been addressed in the present paper, where a full design method for composite cold-formed steel flooring systems has been established.

The prediction of the moment capacity of composite cold-formed steel beams is based on the calculation of the attained degree of partial shear connection, with the magnitude varying between that of the bare steel beam and of the equivalent composite beam with full shear connection. As far as the effective flexural stiffness is concerned, this ranges between the values of flexural stiffness of the corresponding systems with zero and full interaction at the beam-board interface and its calculation is based on the shear bond coefficient of the connection. The presented design predictions were compared against results reported in the literature [4,5]. The mean and COV values of the ratios of the moment capacities predicted by the design proposal over those attained in 12 physical tests [4] and 78 numerical simulations [5] are 0.92 and 0.06, respectively, while the equivalent ratios for flexural stiffnesses are 1.00 and 0.04, respectively.

The proposals made herein enable considerably enhanced structural efficiency to be achieved in cold-formed steel flooring systems through the harnessing of composite action while establishing practical and accurate design rules for composite floors comprising cold-formed

steel beams and wood-based particle boards, which are suitable for use in practice and incorporation into future revisions of structural design standards.

Acknowledgements

The authors are grateful to Ayrshire Metal Products for their financial and technical contributions to the project.

References

[1] DJ Oehlers, MA Bradford, Composite Steel and Concrete Structural Members. Fundamental Behaviour, Pergamon, Great Britain, 1995.

[2] JWB Stark. Composite steel and concrete beams with partial shear connection, Heron. 34 (1989) 1-63.

[3] RP Johnson, IM May. Partial-Interaction Design of Composite Beams, Struct.Eng. 53 (1975) 305-311.

[4] P Kyvelou, L Gardner, DA Nethercot. Testing and analysis of composite cold-formed steel - wood-based flooring systems, Journal of Structural Engineering. 143 (2017) 04017146 (16pp).

[5] P Kyvelou, L Gardner, DA Nethercot. Finite Element Modelling of Composite Cold-Formed Steel Flooring Systems, Engineering Structures. [submitted] (2017).

[6] Rocky Mountain Structural Floors, Steel Joist & OSB, (2017).

[7] EN 1994-1-1, Eurocode 4. Design of composite steel and concrete structures. General rules and rules for buildings, European Committee for Standardization, Brussels, 2005.

[8] EN 1993-1-3, Eurocode 3. Design of steel structures. Part 1-3: General rules - Supplementary rules for cold-formed members and sheeting, European Committee for Standardization, Brussels, 2006.

[9] EN 1993-1-1, Eurocode 3. Design of steel structures. General rules and rules for buildings, European Committee for Standardization, Brussels, 2005.

[10] EN 1995-1-1, Eurocode 5: Design of timber structures. Part 1-1: General — Common rules and rules for buildings, European Committee for Standardization, Brussels, 2004.

[11] RP Johnson, Composite Structures of Steel and Concrete. Beams, Slabs, Columns, and Frames for Buildings, Third ed., Blackwell Publishing 2004.

[12] EN 1993-1-5, Eurocode 3. Design of steel structures. Part 1-5: Plated structural elements, European Committee for Standardization, Brussels, 2006.

[13] SCI, Shear Connection in composite beams, Advisory Desk. AD 266 (2003).

[14] RP Johnson, D Anderson, Designers' Guide to EN 1994-1-1 Eurocode 4: Design of composite steel and concrete structures Part 1.1: General rules and rules for buildings, Thomas Telford Publishing, 1 Heron Quay, London, 2004.

[15] CG Coughlan, Minimum degree of shear connection rules for UK construction to Eurocode 4, P405 (2015).

[16] R Bartschi, Load-Bearing Behaviour of Composite Beams in Low Degrees of Partial Shear Connection, Swiss Federal Institute of Technology, Zurich, Switzerland, 2005.

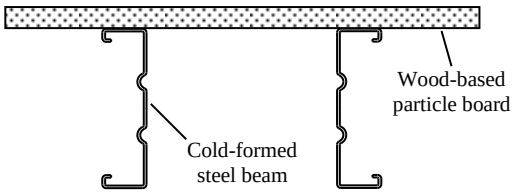
[17] H Kreuzinger, Mechanically jointed beams and columns, in: Blass HJ, Aune P, Choo BS, Gorlacher R, Griffiths DR, Hilson BO, et al. (Eds.), Timber Engineering. STEP 1. Basis of design, material properties, structural componets and joints. Centrum Hout, The Netherlands, 1995.



(a) Overall view [6]

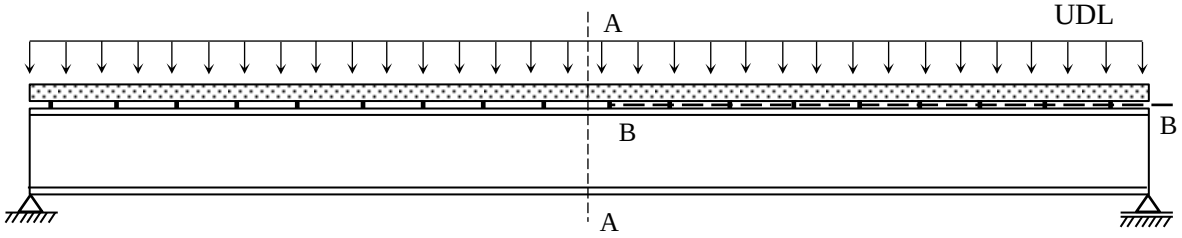


(b) Side view [4]

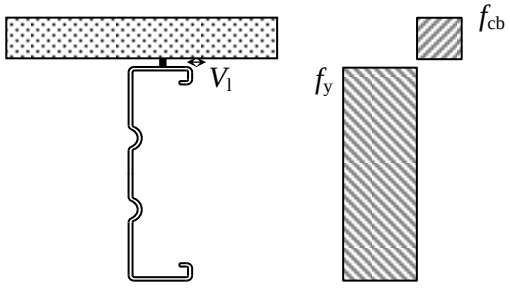


(c) Cross-section [4]

Figure 1: Composite cold-formed steel flooring systems



(a) Critical cross-sections along the length of a composite beam under uniform distributed load

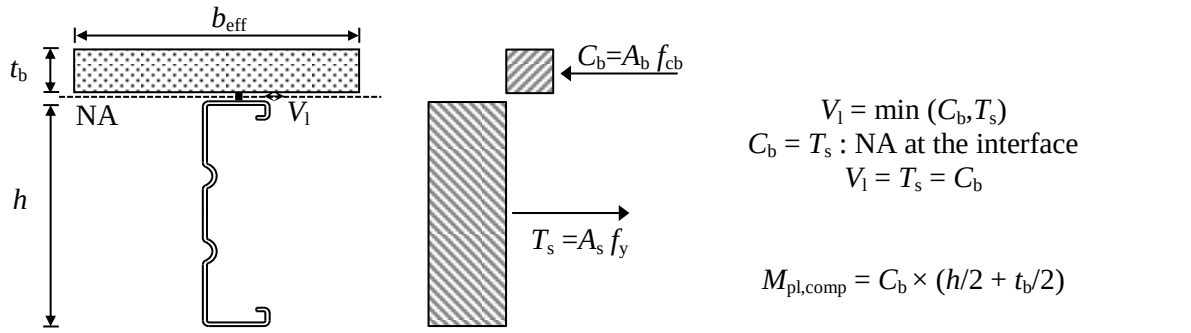


(b) Bending failure at cross-section A-A

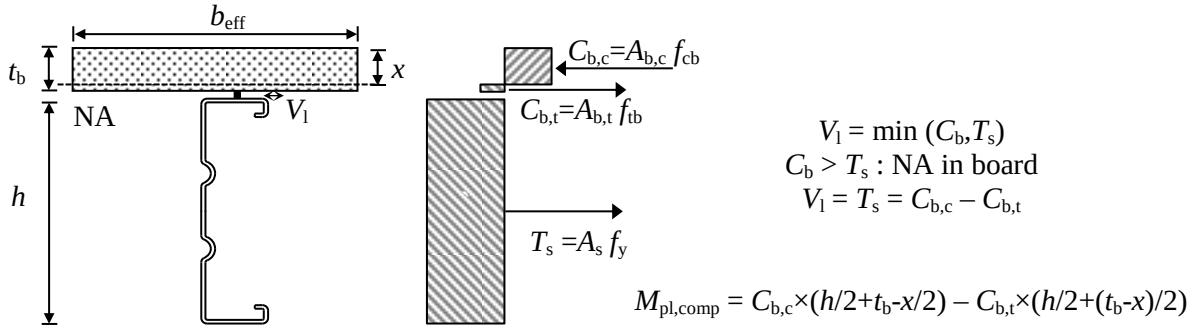


(c) Failure of connection along cross-section B-B

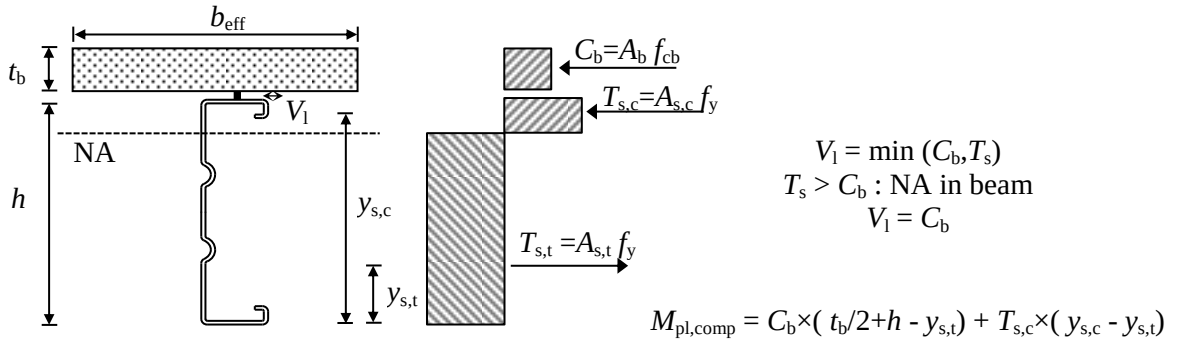
Figure 2: Critical cross-sections and modes of failure of composite beam



(a) Neutral axis at the beam-board interface



(b) Neutral axis in the floorboard



(c) Neutral axis in the steel beam

Figure 3: Longitudinal force transferred by the shear connection for a composite system with full shear connection

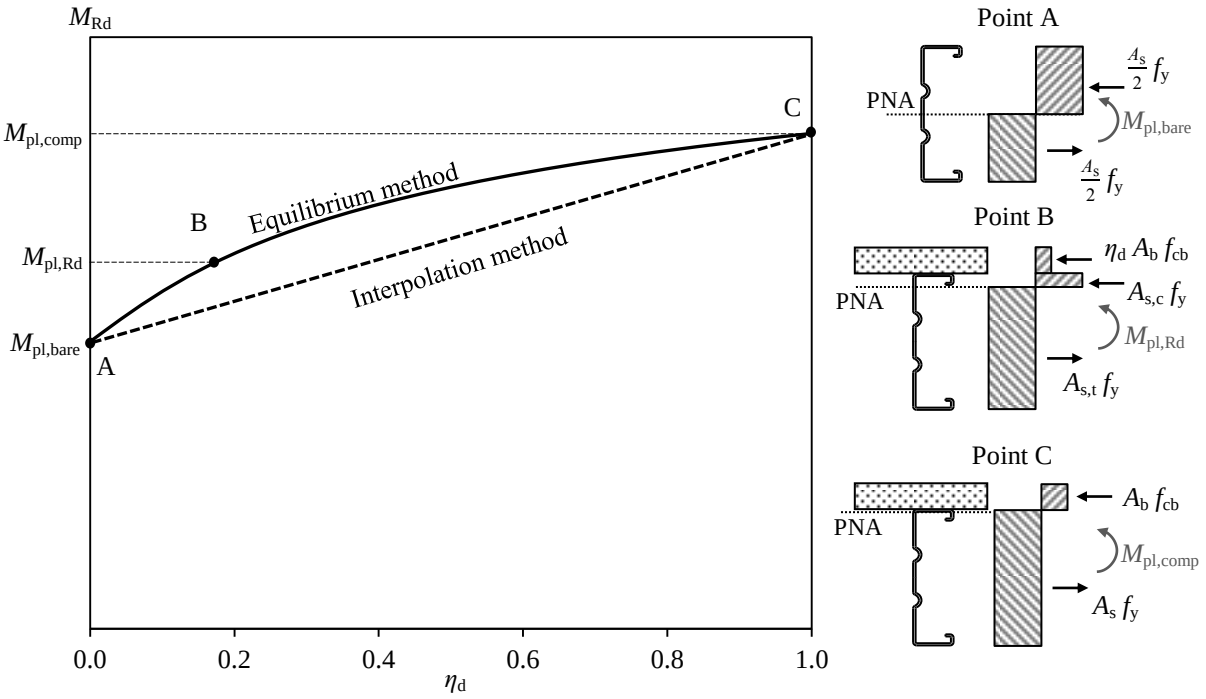


Figure 4: Variation of moment capacity of conventional composite systems with attained degree of shear connection η_d according to EN 1994-1-1 [5]

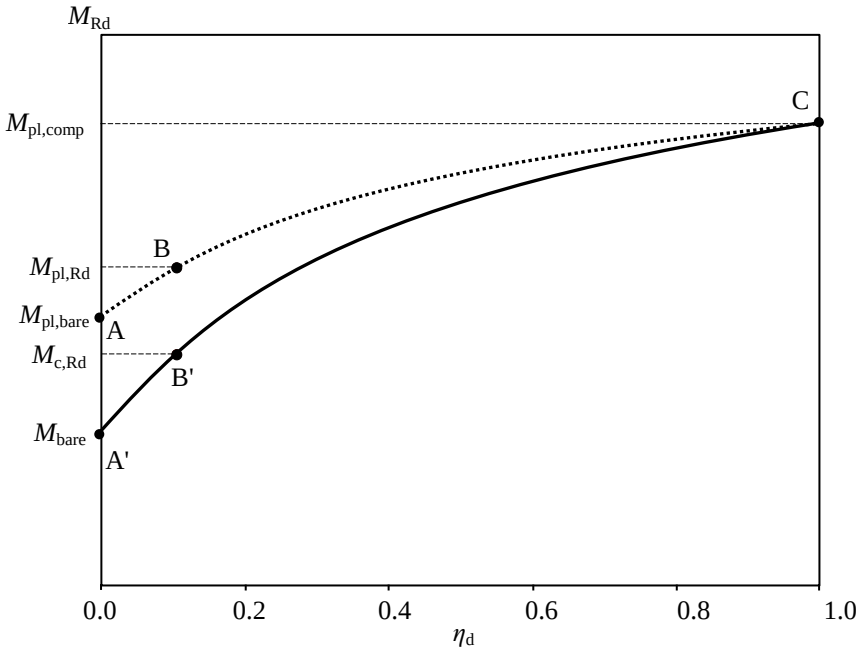


Figure 5: Variation of moment capacity of cold-formed composite systems against attained degree of shear connection η_d according to the proposed design method

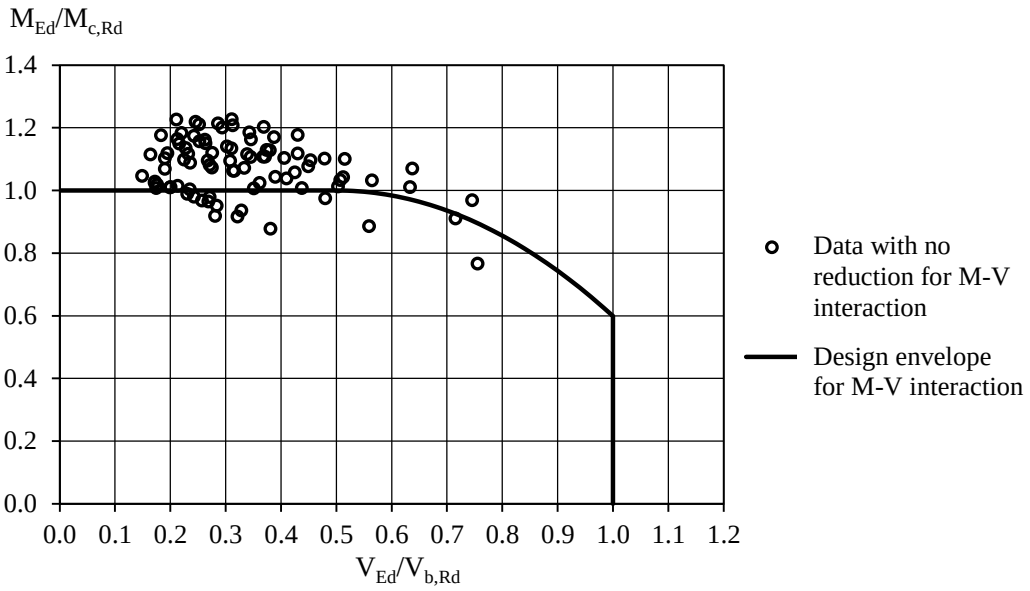


Figure 6: Interaction between bending and shear

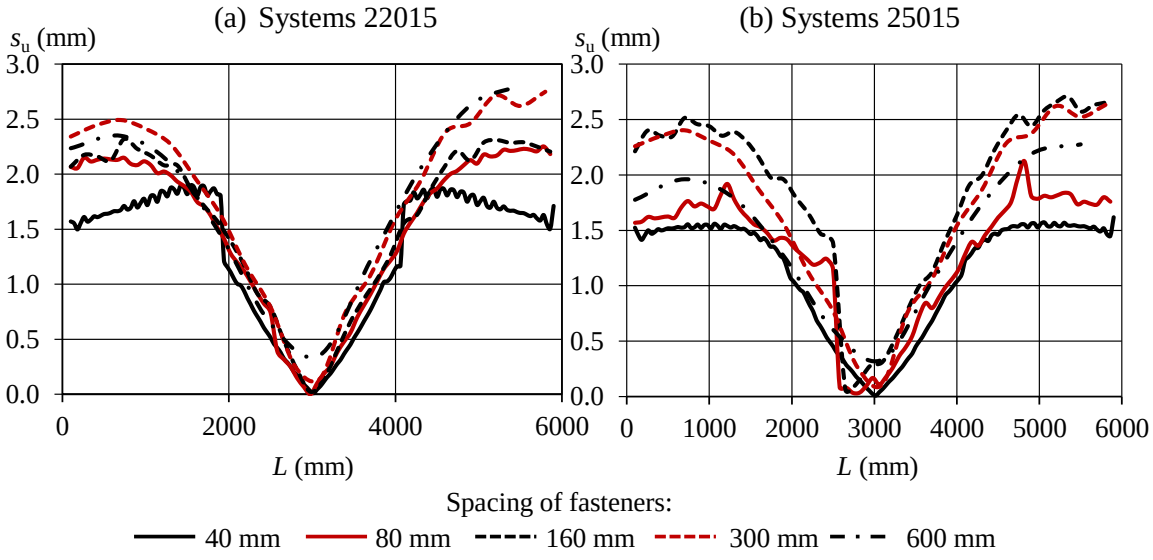


Figure 7: Slip of connectors along the length of the beam

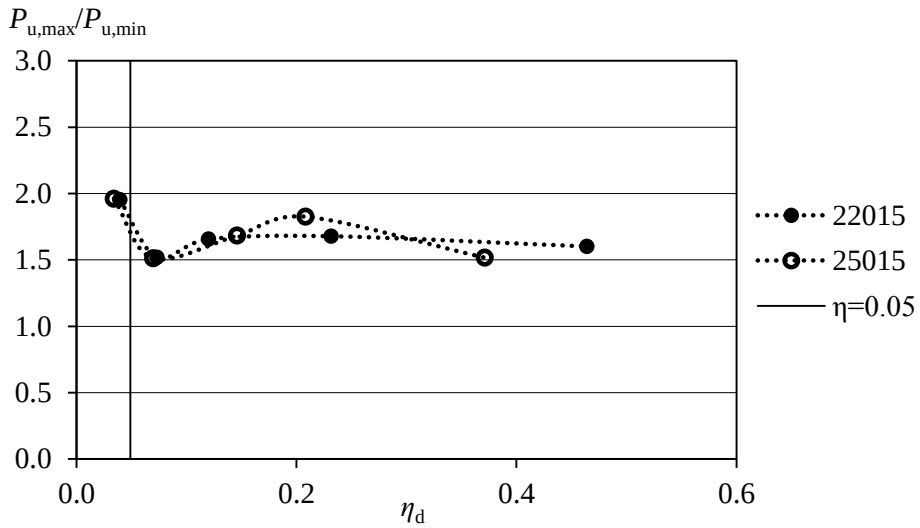


Figure 8: Ratio of maximum to minimum force in shear connectors in the critical lengths with increasing degree of shear connection

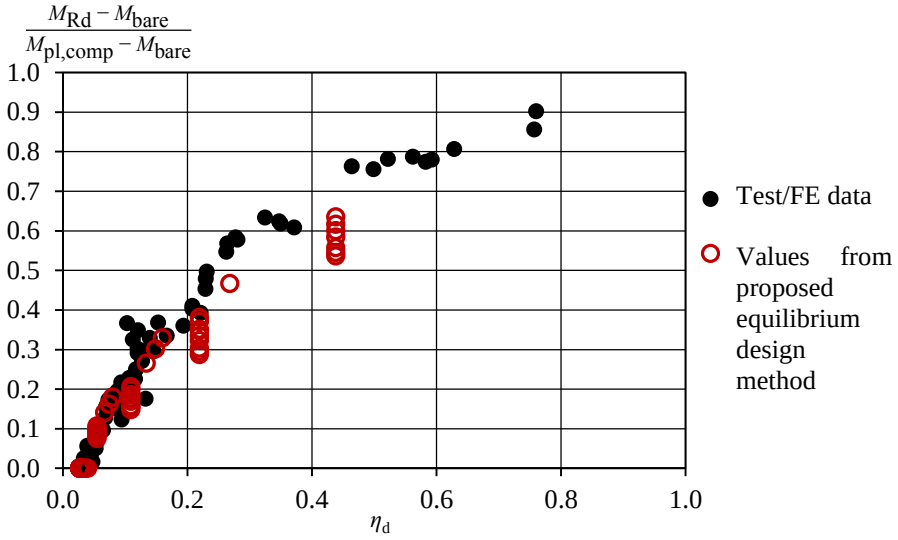
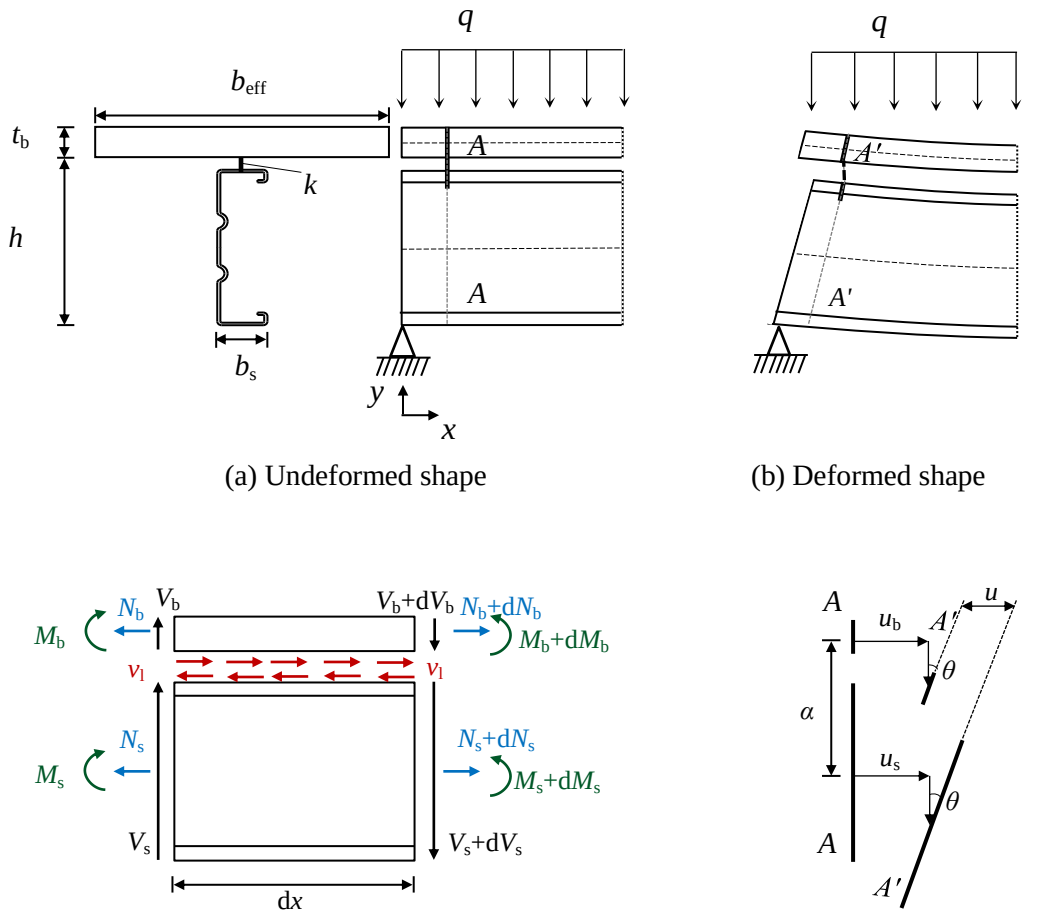


Figure 9: Comparison of predicted and observed gains in moment capacity with increasing degree of shear connection



(a) Undeformed shape

(b) Deformed shape

(c) Cross-sectional equilibrium of an incremental element

(d) Deformation of cross-section A-A to A'A'

Figure 10: Deformations and element equilibrium in composite beam subjected to vertical load

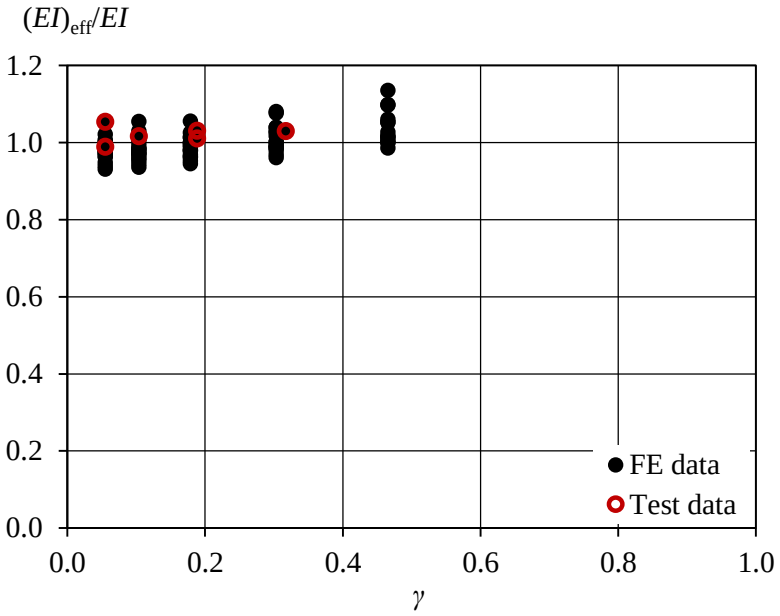


Figure 11: Comparison between values of flexural stiffness obtained from the proposed design method and from the experimental and numerical investigations

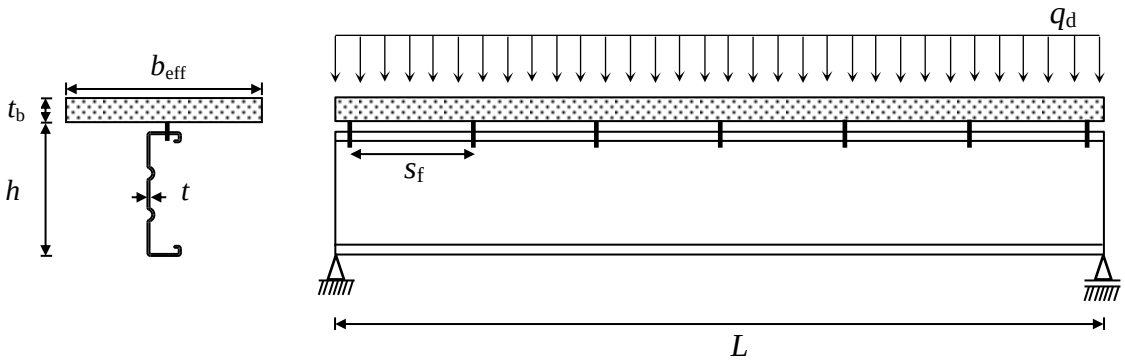


Figure 12: Examined flooring system for worked example

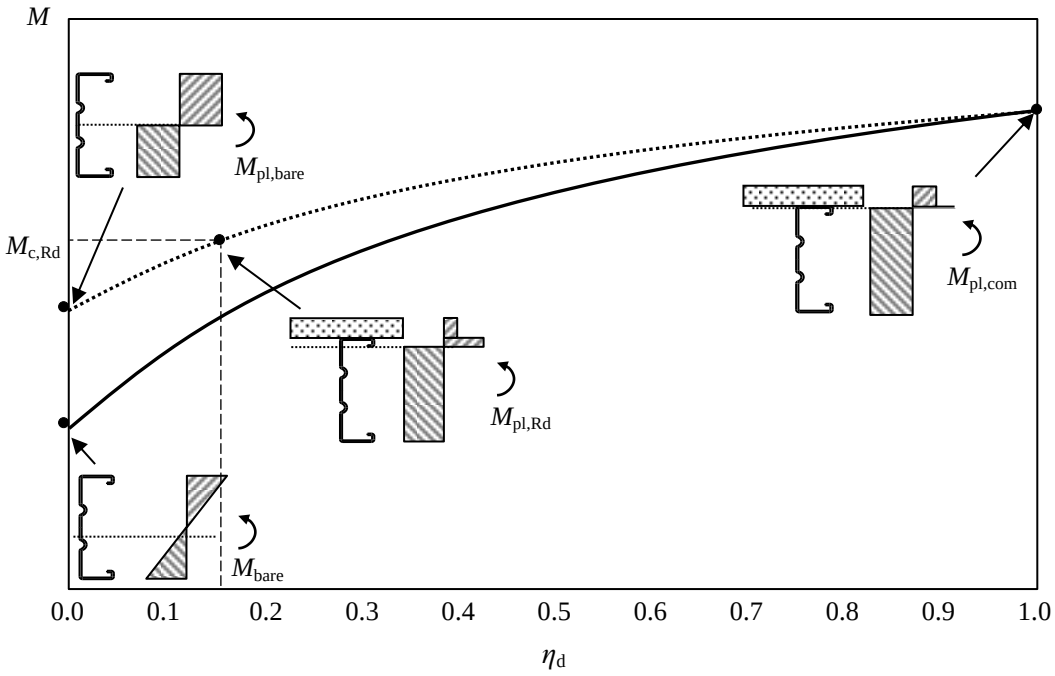


Figure 13: Moment capacities required for the calculation of the moment resistance of the composite system $M_{c,Rd}$

Table 1: Summary of comparisons of values of moment resistance and flexural stiffness between the proposed design method and data obtained from numerical simulations and physical tests (of number n)

	s_f (mm)	M_{Rd}/M_u	$M_{lin,Rd}/M_u$	$(EI)_{eff}/EI$
FE results n = 80	600	0.95	0.95	0.98
	300	0.93	0.88	0.98
	160	0.90	0.82	0.99
	80	0.90	0.79	1.01
	40	0.91	0.83	1.03
Test results n = 10	600	0.96	0.96	1.02
	300	0.94	0.92	1.02
	150	0.87	0.81	1.02
	75	0.85	0.81	1.03
	AVERAGE	**0.91**	**0.86**	**1.01**
	COV	**0.04**	**0.07**	**0.02**

Table 2: Geometrical and material characteristics of the steel beam

Height :	h =	250	mm
Thickness :	t =	1.5	mm
Length :	L =	6000	mm
Area :	A_s =	655.7	mm^2
Second moment of area :	I_s =	5.75×10^6	mm^4
Yield strength :	f_y =	490.5	MPa
Elastic modulus :	E_s =	201000	MPa

Table 3: Geometrical and material characteristics of floorboards

Effective width :	b_{eff} =	600	mm
Thickness :	t_b =	38	mm
Area :	A_b =	22800	mm^2
Second moment of area :	I_b =	2.74×10^6	mm^4
Compressive strength :	f_{cbd} =	9.92	MPa
Elastic modulus :	E_{bd} =	1769	MPa

Table 4: Geometrical and material characteristics of fasteners

Diameter :	d =	5.50	mm
Threaded diameter :	d_{thr} =	4.13	mm
Spacing of fasteners :	s_f =	300	mm
Ultimate tensile strength :	f_u =	720	MPa
Slip modulus :	K_o =	1206	N/mm